Orbital
The electronic journal of chemistry

the electronic journal of chemistry

Full Paper | http://dx.doi.org/10.17807/orbital.v13i5.1555

Remaining Capacity Estimation of Lead-acid Batteries Using Exponential Decay Equations

Luiz Alberto Vicari * [a], Vanderlei Aparecido de Lima [b], Alex Silva de Moraes [c], and Mauro Chierici Lopes [c]

The precise capacity estimation of batteries can extend their lifespan and is necessary to ensure reliability and safety of operation. Many methods have been developed with this objective in the last decades. However, there is still research for more accurate and less complex methods in order to estimate the state of charge of operating batteries. This article presents exponential decay equations that model the behavior of the battery capacity drop with the discharge current. Experimental data for different application batteries showed that these equations have a superior accuracy compared to the empirical Peukert equation. Their parameters are dimensionally coherent and make the characterization and categorization of batteries possible, besides, they give insights about the behavior of the electrodes under different discharge rates. Due to the low complexity and easy adaptability to the currently employed methods, these equations can be easily employed in battery management systems without the need for great computational power.

Graphical abstract

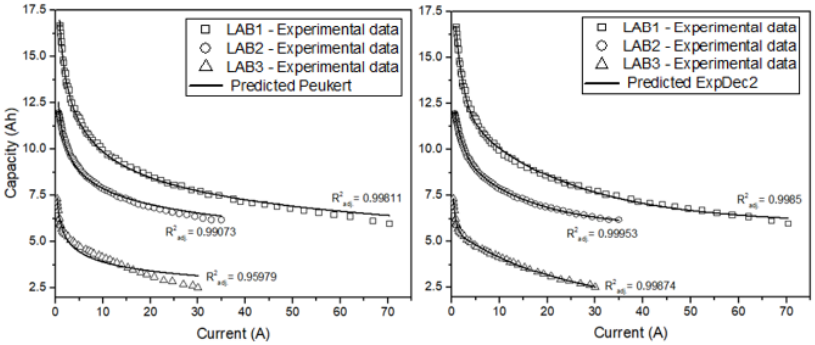

Keywords

Ah counting
Battery management systems
Capacity estimation
Lead-acid batteries
State of charge

Article history

Received 01 October 2020
Revised 12 Feb 2021
Accepted 06 Oct 2021
Available online 27 December 2021

Handling Editor: Cauê A. Martins

1. Introduction

In search of reducing greenhouse gas emissions, electrochemical technologies play an important role in the storage of intermittently generated energy from wind and solar farms. Compared to other energy storage technologies, electrochemical systems have higher thermodynamic efficiency because they convert chemical energy directly into electricity in addition to a short response time and lower environmental footprints [1]. Furthermore, batteries are widely employed in uninterruptible power supplies, in the propulsion of traction equipment, forklifts, and passenger cars. The lead-acid battery (LAB) has been widely used in a lot of those systems because it offers an acceptable combination of

[a] Instituto Federal de Educação, Ciência e Tecnologia de Santa Catarina, Campus São Lourenço do Oeste, 89990-000, São Lourenço do Oeste, SC, Brazil. [b] Universidade Tecnológica Federal do Paraná, Campus Pato Branco, 85503-390, Pato Branco, PR, Brazil. [c] Universidade Estadual do Centro Oeste do Paraná, Campus CEDETEG, 85040-167, Guarapuava, PR, Brazil. * Corresponding author. E-mail: **luiz.vicari@ifsc.edu.br**

performance parameters within lower costs compared to other battery chemistries [2-4]. Service reliability and safety of stand-alone batteries or battery grids depend on the accurate prediction of their state of charge (SOC). In addition, the service life of a battery can be extended with proper management of its cycling regime which ultimately depends on predicting the state of charge [5-10]. The SOC expresses the remaining capacity, C_r, of a partially discharged battery as a percentage of the fully charged battery, C_{full}:

$$SOC = \frac{C_r}{C_{full}} \times 100\% \quad (1)$$

However, the full charge capacity decreases over time, depending on the operating temperature, the electrolyte concentration, the history of charging and discharging cycles, among other conditions that lead to its aging [4]. Since the capacity is strongly dependent on the discharge current, the definition above implicitly assumes that C_r and C_{full} are evaluated at the same discharge current as the nominal capacity, C_{nom}, which is defined by the manufacturer. This is done by a laboratory test through a discharge under a constant current, I_d, until the battery voltage reaches some specified cut-off voltage. If the discharge test lasts t_d hours and I_d is expressed in amperes, then the battery capacity is equal to $I_d \times t_d$ ampere-hours (Ah), and the corresponding SOC can be calculated [8]. The applicability of this definition is limited by its ex-situ nature and by the fact that the actual operation conditions involve variable discharge current not necessarily comparable to the discharge test current. Due to the importance of SOC estimation for battery management, many methods have been developed [9] to circumvent these limitations. These methods present some disadvantages for practical uses. Open circuit measurements require the removal of operation, impedance spectroscopy is onerous, and "coup de fouet" mapping, neural networks [5], Fuzzy logic and Kalman filters [11-13] have high computational cost. Among the various methods for estimating SOC, one of universal applicability is Ah counting, which consists in tracking the input and output of charge on the battery. The SOC at time t, SOC_t, can be expressed through equation [13-15]:

$$SOC_t = SOC_{t_0} + \frac{\int_{t_0}^{t} I_\tau d\tau}{C_{nom}} \quad (2)$$

where, SOC_{t_0} is the initial SOC, I is the magnitude of the current, being positive for a charge current and negative for a discharge current. Equation (2) assumes a capacity independent of the discharge current. In a real battery, however, irreversible processes occur leading to a drop of capacity, which is greater the higher the discharge current. Therefore, the remaining capacity, measured at constant discharge current, decreases for greater discharge rates. The empirical Peukert equation is widely employed to model this behavior:

$$C_r(I_d) = K \times I_d^{(1-n)} \quad (3)$$

where K and n are empirical parameters dependent on the battery technology with n, known in the literature as Peukert coefficient, varying between 1.1 and 1.3. Parameter K indicates the degree of nonideality of the battery and is equal to 1 for an ideal battery [4,16]. K is related to the capacity of an ideal battery because, since in that case n equals 1, the right side of equation (3) reduces just to K and is equal to C_r, which is now independent of the discharge current. Furthermore, in this case, the battery uses its total available capacity [17]. However, $n>1$ for real batteries and, the greater n is, the more dependent C_r is on the discharge current. In this sense, n is related to the efficiency of the battery [4].

Doerffel and Sharkh [17] have reviewed different Ah counting implementations based on Peukert equation to quantify the remaining capacity under actual operating conditions. They concluded that the use of Peukert equation under conditions with a variable discharge current and changing operating temperature results in an underestimation of the remaining capacity. Several authors have criticized the dependence of Peukert parameters on the operating conditions and the battery SOC [16-23]. Cugnet et al. [21] pointed out that the accuracy of Peukert equation is limited by the discharge rate range and the choice of cut-off voltage. Another pitfall of the Peukert equation is the lack of physical meaning owing to its imbalance in physical quantities [20,24] and the prediction of an infinite capacity when the discharge current tends to zero [19,21,23].

The lack of physical meaning happens because, since in equation (3) the $I_d^{(1-n)}$ term as units of $A^{(1-n)}$, K must have units of hA^n, in order for the product to have units of capacity (Ah). Therefore, the units of K depend on the parameter n and are physically inconsistent. This is a disadvantage of Peukert equation which does not appear in exponential decay equations that describe the capacity of batteries.

In this article, we compare the accuracy of Peukert equation with three exponential decay equations. These equations are more accurate than Peukert equation and have dimensionally consistent parameters, which can be useful to characterize and categorize batteries. Furthermore, they can give insights about the behavior of phenomena that lead to the drop in the batteries capacity.

2. Material and Methods

From the set of Peukert plots, obtained from datasheets of 20 LABs, operating at temperatures of 25 °C, presented by a manufacturer (which is available in the first **supplementary material** of this paper), that were digitalized, and a set of the capacity for different discharge currents presented in a patent [25], we calculated the parameters of the Peukert equation and of the three exponential decay equations presented below:

$$C_r(I_d) = C_0 + C_1 \exp\left(\frac{-I_d}{I_{C_1}}\right) \quad (4)$$

$$C_r(I_d) = C_0 + C_1 \exp\left(\frac{-I_d}{I_{C_1}}\right) + C_2 \exp\left(\frac{-I_d}{I_{C_2}}\right) \quad (5)$$

$$C_r(I_d) = C_{max} \exp\left[-\left(\frac{-I_d}{I_C}\right)^a\right] \quad (6)$$

where, in equations (4), one-phase exponential decay (ExpDec1), and (5), two-phase exponential decay (ExpDec2), C_0 (Ah) is the part of the capacity that is not sensitive to the discharge current, C_1 and C_2 (Ah) are the amplitudes of the parts of the capacity that decay exponentially with the

discharge current at a rate determined by the characteristic currents I_{C_1} and I_{C_2}(A), and, in equation (6), stretched exponential, C_{max} (Ah) is the capacity when the discharge current tends to zero, I_C (A) is a characteristic current and, together with the exponent a, they dictate the dynamics of the decay.

Datasheets of different application LABs were analyzed, and the accuracy of the empirical equations were evaluated quantitatively from the dispersion between their capacity estimates and the experimental results by the chi-square test, *χ2*, and by the Akaike information criterion (AIC). The lower the *χ2* and AIC values, the higher the prediction accuracy. The AICs of the Peukert adjustments were obtained without data linearization, as usual. However, this does not lead to damage to its accuracy. We describe the results of three different application LABs and of the patent battery. The results of the other LABs are presented in the second **supplementary material**.

Additionally, we simulated the cells of a 60 Ah flooded LAB and a LAB pack in COMSOL Multiphysics® using a model based on the LAB presented by Cugnet et al. [27][26], composed of 6 cells. We compared the adjustment of Peukert equation and the equation proposed by D'Alkaine et al. [23] for the behavior of both the capacities of the cells (6 cells in series without taking into account the ohmic resistance) and the capacities of the LAB pack (6 cells in series taking into account the ohmic resistance).

3. Results and Discussion

Fig. 1a presents the Peukert plot for three different capacity and application LABs. LAB1 (17Ah) is used as main and standby power supplies, LAB2 (12 Ah) as standby power supplies, and LAB3 (7.2 Ah) is used for pitch backup systems in wind turbines. This plot is represented by the axes $\log(t_d)$ and $\log(I_d)$, where parameters K and $-n$ from Peukert equation are, respectively, the linear and the angular coefficients.

Although the fit is good in these coordinates, since the statistical correlation based on the number of independent variables, R^2_{adj}, are approximately 1, the logarithm transformation leads to a compression of the data that tend to be distributed in a straight line. Nevertheless, small deviations can be seen, particularly in the pitch backup systems in wind turbines LAB, mainly at high discharge currents. This way, the Peukert parameters are strongly dependent on the discharge range that they are calculated. Fig. 1b shows the LAB capacities as a function of the discharge current, calculated using Peukert equation. It can be seen that the small deviations shown in Fig. 1a become considerably larger, leading to not so accurate LAB capacity and remaining capacity predictions. In general, Peukert underestimates the capacity at intermediate currents and overestimates it at low and high currents. At very low currents, the deviation is even larger, since Peukert predicts an infinite capacity at currents tending to zero.

It is instructive to compare the behavior of the capacity of the LAB cells and of the LAB. Fig. 2 shows this comparison. The capacities of the cells were taken at constant cut-off voltage of 10.5V. The LAB voltages were obtained by subtracting all ohmic losses (in the connections, between the cells and the battery terminals, and in the grids that support the active material and lead the current to the connections) from the voltage of the cells. This way, the battery reaches the cut-off voltage faster than the cells, leading to a lower capacity. However, like the studies mentioned above and practice in battery tests, we used variable cut-off voltages in our simulations. The higher the discharge current, the lower the cut-off voltage used.

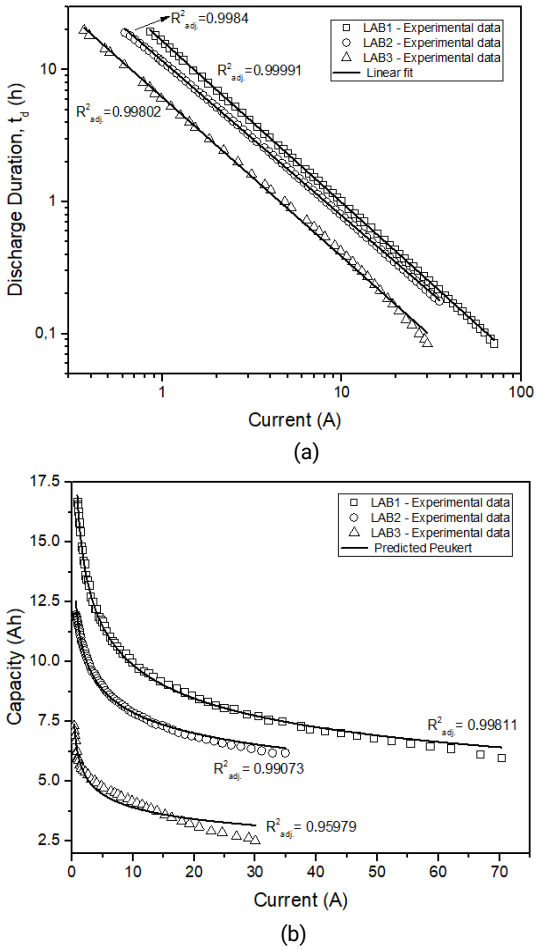

Fig. 1. Comparison of Peukert predictions (a) with data linearization and (b) without linearization.

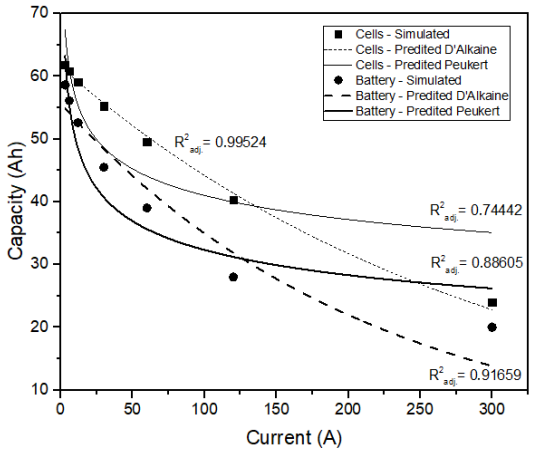

Fig. 2. Capacities of 6 cells (without ohmic resistance) and 60 Ah flooded battery (cells with ohmic resistance), obtained from simulation and predictions by two models from the literature.

D'Alkaine et al. [23] studied the behavior of the capacity of the positive electrode of a LAB in excess of electrolyte and low discharge currents and proposed an exponential decay equation for the capacity. For the simulated cells this equation presented better adjustment than the Peukert equation.

However, it must be considered the observation of Vervaet and Baert [22] that, due to the small range and few measurements carried out in D'Alkaine et al. [23] tests, it is not possible to assert that this representation is better than Peukert's for LABs.

For the simulated LAB the estimates of Peukert equation improve, while the estimates through D'Alkaine equation lose accuracy, since D'Alkaine et al. do not take into account the ohmic losses. The greatest deviations on Peukert predictions for the simulation are due, in part, to two factors. First, to the greater range of discharge currents used in the simulations ($C_{nom}/20$ to $5C_{nom}$, while in the battery tests the discharges were of $C_{nom}/20$ to $4C_{nom}$ at the most). Second, to the cut-off voltage choice. As pointed out in [21], the appropriate choice of the cut-off voltages is important for the obtainment of Peukert parameters. In Fig. 2, at a discharge current of 300 A, the battery capacity approaches the cell capacity because the cut-off voltage point where the two capacities are approximately the same.

It is noteworthy that when the capacities are taken at different cut-off voltages, the real reference of the battery capacity is lost. In practice, the choice of the cut-off voltage is, in general, heuristic. Therefore, it is possible to obtain a better adjustment of the parameters by establishing cut-off voltages that are more suitable for the model used. Anyway, Peukert equation seems to capture both the diffusive phenomenon [22] and the ohmic resistance of the battery components. Therefore, it describes better the LAB behavior.

Fig. 3a–3c show the capacity predictions of the three exponential decay equations. With one more parameter than Peukert, equation (4), ExpDec1, also overestimates the capacity at high currents and underestimates it at intermediate currents, however, when the current tends to zero, it predicts a limiting capacity. Equation (5), ExpDec2, has a better fitting than the previous equations in the entire discharge range, which is expected, since it has more parameters. Equation (6), stretched exponential, with only three parameters, adjusts well to the measured capacities in the entire discharge range.

Table 1 shows the accuracy of the different equations by the measurement of the dispersion between the estimate and the experimental data by the $\chi 2$ test and by the AIC. Lower values of $\chi 2$ and AIC indicate better adjustment of the estimates to the experimental data. AIC penalizes equations with a higher number of parameters. Therefore, the equation with a lower dispersion sometimes has a higher AIC. This is the case of the LAB3, where the ExpDec1 leads to a dispersion that is lower than Peukert's, however, its AIC is higher due to a penalty because of the additional parameter compared to Peukert. The data presented in the supplementary material corroborates the observations for the three LABs presented here. Peukert and ExpDec1 have equivalent accuracy in most cases. Occasionally, the accuracy of one or the other loses quality. This is the case of ExpDec1 in LAB1, where the estimate from approximately 40 A presents an increase in dispersion, which indicates that the power of prediction can vary significantly according to the LAB. Equations ExpDec2 and stretched exponential have superior accuracy compared to the other two. This is an important aspect for the Ah counting, because during the integration, the errors accumulate and little distortions can lead to great deviations during the discharge.

Table 2 presents the capacity estimation of all four equations studied under different discharge currents and the error of each one of them with respect to an experimental LAB [25], where C_{Exp} is the experimental LAB capacity, C_P is the Peukert capacity, and C_{E1}, C_{E2} and C_{St} are the capacities of equations (4), (5) and (6), respectively. The tendency of Peukert's overestimation of the capacity at low and high currents and its underestimation at intermediate currents is clear. For this LAB, the ExpDec1 accuracy is much higher than Peukert's, corroborating what was said previously that the power of prediction varies significantly depending on the LAB. In this case, its accuracy is equivalent to the stretched. ExpDec2, with smaller errors, shows great adherence to the experimental results and no tendency to over or underestimate the capacity within this discharge current range. Added to its prediction accuracy independent of the battery type, this characteristic makes this equation very reliable to be employed in Ah counting.

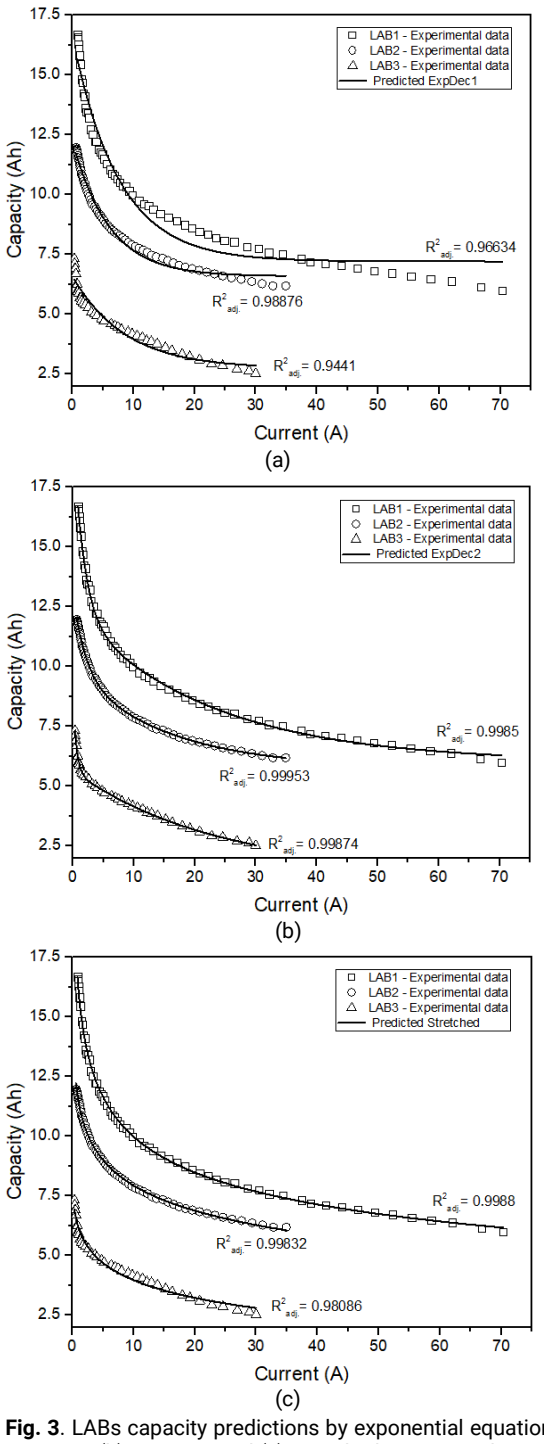

Fig. 3. LABs capacity predictions by exponential equations, (a) ExpDec1, (b) ExpDec2 and (c) stretched exponential.

Table 1. Capacity estimation accuracy of all 4 equations for LABs 1 to 3.

Empirical Model	LAB1		LAB2		LAB3	
	$\chi 2$	AIC	$\chi 2$	AIC	$\chi 2$	AIC
Peukert	0.132	-250.3	0.221	-241.9	0.771	-106.3
ExpDec1	2.052	-64.7	0.307	-227.0	0.723	-91.1
ExpDec2	0.087	-261.2	0.010	-449.2	0.016	-247.3
Stretched	0.059	-278.1	0.038	-316.7	0.285	-136.1

Besides the power of prediction of the empirical equations, the physical meaning of their parameters can help to better understand the LAB behavior. Table 3 presents the equation parameters normalized by the C_{nom} (except parameters n and a, which are dimensionless). As mentioned before, Peukert parameters n and K are related, respectively, to the battery's efficiency and to its capacity. However, since the dimensionality of K is coupled to n, it is not possible to interpret its meaning, leaving only the indication of the battery's efficiency by n.

Table 2. Capacity estimation accuracy of all 4 equations for the 50 Ah LAB.

I_d (A)	C_{Exp} (Ah)	C_P (Ah)	Error %	C_{E1} (Ah)	Error %	C_{E2} (Ah)	Error %	C_{St} (Ah)	Error %
5	50.3	54.9	9.2	49.6	-1.4	50.3	-0.1	50.9	1.2
10	47.1	46.7	-0.9	47.2	0.2	47.2	0.1	46.6	-1.2
20	42.2	39.7	-6.0	42.9	1.7	42.2	0.1	41.5	-1.6
40	35.9	33.7	-6.1	36.4	1.4	35.8	-0.3	35.8	-0.2
60	31.8	30.6	-3.7	31.9	0.4	31.8	0.2	32.3	1.5
80	29.2	28.6	-1.9	28.8	-1.3	29.2	0.0	29.7	1.6
100	27.1	27.2	0.3	26.7	-1.6	27.3	0.6	27.6	1.8
120	25.9	26.0	0.5	25.2	-2.8	25.7	-0.7	25.9	0.0
160	23.4	24.3	4.0	23.4	0.1	23.4	0.2	23.3	-0.6
200	21.8	23.1	5.9	22.6	3.7	21.8	0.0	21.2	-2.7
$\chi 2$		0.863		0.091		0.003		0.065	
AIC		21.3		3.1		-8.6		0.7	

Table 3. Parameters of the empirical equations.

Empirical Model	Normalized Parameter	LAB1	LAB2	LAB3
Peukert	K	0.963	0.964	0.845
	n	1.220	1.167	1.191
ExpDec1	C_0	0.424	0.549	0.380
	C_1	0.557	0.475	0.539
	I_{C_1} (h^{-1})	0.442	0.500	1.203
	$C_0 + C_1$	0.981	1.023	0.919
ExpDec2	C_0	0.354	0.479	0.186
	C_1	0.447	0.272	0.468
	I_{C_1} (h^{-1})	0.101	0.168	0.074
	C_2	0.369	0.336	0.598
	I_{C_2} (h^{-1})	1.327	1.305	3.261
	$C_0 + C_1 + C_2$	1.170	1.087	1.252
Stretched	C_{max}	11.091	2.108	1.327
	I_C (h^{-1})	5.8E-07	0.343	2.120
	a	0.078	0.167	0.305

In ExpDec1, C_0 can be interpreted as the part of the capacity that is independent of the current, that is, the capacity that the battery would deliver even at high discharge currents. Under high current conditions there is not enough time for the electrolyte to penetrate the electrode pores. In LABs when the capacity is limited by the positive electrode, then the parameters of the equations relate more strongly to the properties of this electrode. Therefore, this capacity is equivalent to the amount of active material of the positive electrode that would react if the electrolyte were already present inside its pores. C_1 is the fraction of the capacity that is sensitive to the discharge current, whose decay dynamics is dictated by I_{C_1}. More specifically, I_{C_1} is the discharge current at which C_r is $C_0 + C_1/e$, where e is the Euler number. When I_d tends to zero, the capacity is the sum of C_0 and C_1. Under this condition, the diffusion is not limiting for the innermost part of the active material consumption, which means that all active material available is consumed. That is why its sum is close to unity. It is noteworthy that I_{C_1} for LAB3 is considerably larger than for LABs 1 and 2. This is due to the fact that LAB3 is used for pitch backup systems in wind turbines, as mentioned above, and, therefore, is projected to operate under high currents for short periods of time. On the other hand, LABs 1 and 2 are used as main and standby power supplies, hence, they are projected to operate under moderate currents for longer periods of time.

For ExpDec2, C_0 can be interpreted in the same way as for ExpDec1. However, considering ExpDec2 accuracy, its estimation of C_0 must be more precise and coherent with the

given interpretation. Fig. 4 shows two very distinct capacity drop phases that compose the two terms of the exponential decay. This indicates that there are two phenomena or dynamics ruling the drop in the LABs capacity. One possible explanation for this behavior considers the inhomogeneous utilization of the active material through the electrodes. This is shown by Bode [27], where at the end of discharges the distribution of $PbSO_4$ formed varies along the thickness of the electrodes according to the discharge current. For small discharge currents this distribution is quite homogeneous, and as the current increases, less sulfate is produced in the internal part of the electrodes, while in the external part of it, this content almost does not change. This is due to the decrease of the electrolyte concentration in the electrodes, which at higher discharge rates is not replaced in the amount that it is consumed due to diffusional limitations. Since the content of sulfate produced is directly proportional to the capacity of the battery, it is reasonable to infer that the first phase of the decay in ExpDec2, determined by C_1 and I_{C_1}, represents the innermost part of the electrode, which is more sensitive to the discharge current; and the second phase, given by C_2 and I_{C_2}, to its outermost part. The pores morphology dictates the tortuous path at which the electrolyte is subject during diffusion in these media. Therefore, since the parameters of ExpDec2 depend on the diffusion, they can be used to indirectly quantify it and, consequently, give information about the morphology of the positive electrode. Because C_0 is a representation of the capacity when there is no diffusion, it is related to the volume of electrolyte present in the beginning of discharge and, therefore, to the initial porosity of the electrode, as long as its thickness is known. The relationship between C_0 and the volume of electrolyte and initial porosity is due to the fact that, as explained for ExpDec1, C_0 can be interpreted as the capacity of the battery under high discharge currents, since, in that case, there is no time for the electrolyte to diffuse into the pores. Hence, its value must be related to the initial porosity, which is related to the volume of electrolyte present before the discharge. Furthermore, the predominance of the first phase at low currents corroborates the behavior of only one exponential decay verified by D'Alkaine et al. [23].

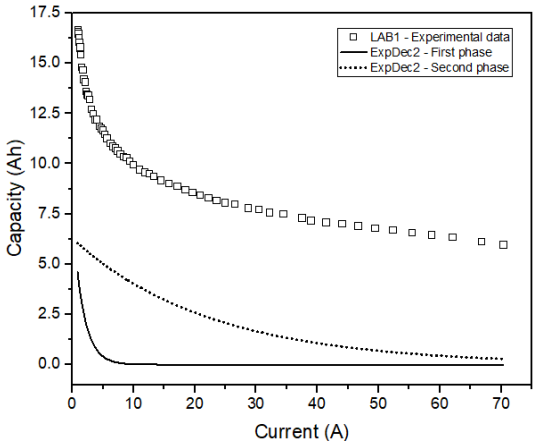

Fig. 4. Distinct exponential decay phases for the ExpDec2.

For these two exponential decay equations, the dimensional coherence of their parameters and the variability inside a narrow range of values can be used to characterize each battery individually. When the parameters are more distinct, they can be useful to categorize the different types of batteries, as is the case of LAB3 when compared to LABs 1 and 2. If the parameters are monitored during the life of the battery, they can help to control the deterioration of its active material. State of health (SOH) diagnostics are also possible based on this. Because it has more parameters, ExpDec2 is more appropriate for the characterization, categorizing and monitoring of LABs aging.

The stretched exponential decay function can be interpreted as a global representation of a system with many independent exponential decays, each with a specific decay rate [28]. Therefore, the parameter I_C can be understood as a characteristic discharge current that reflects the global decay together with the exponent a. As seen previously, both exponential decays of ExpDec2 explain, together, the behavior of the capacity loss of the battery and additional decays, if present, have little relevance. In any case, the stretched exponential decay equation has the merit that, with less parameters than ExpDec2, also represents this behavior well. The stretched exponential presents the characterizing and categorizing properties of the other two exponential decay equations, however, the greater variability of its parameters and the presence of the exponent a complicate its interpretation.

4. Conclusions

Despite the success of Peukert equation, because of its simplicity and acceptable accuracy, its parameters are not very useful to characterize, categorize and monitor the aging of batteries. Exponential decay equations have dimensionally coherent parameters and can be employed for these purposes. The two-phase exponential decay, besides high accuracy, separates clearly the process of loss of capacity with the discharge current into two distinct processes having, therefore, great potential for categorizing and characterizing batteries. Although they have more parameters than Peukert equation, the exponential decay equations are simple enough for their easy implementation in battery management systems for the estimate of both SOC and SOH. The categorization and aging monitoring of the batteries are also easier using the exponential decay equations. The categorization can be made according to the parameters of the equations, since each one is related to a particular physical quantity of interest. The aging monitoring is also possible to be performed by keeping track of the parameters through the lifetime of the battery and comparing them to their initial parameters. The investigation of a greater number of batteries of different applications, with the detailed knowledge of their projects and operating in different temperatures must help to reveal the range of application of these equations in BMS. Furthermore, just like the Peukert equation, the equations presented here can be employed for other battery chemistries.

Supporting Information

We present as a supplementary material the results of other batteries that were not presented in the article.

Acknowledgments

The authors would like to thank Prof. E. C. Pereira, who made the use of the COMSOL Multiphysics® software possible.

Author Contributions

Luiz Alberto Vicari: Conceptualization, Methodology, Investigation, Writing – review & editing. Vanderlei Aparecido de Lima: Methodology, Statistic Analysis. Alex Silva de Moraes: Methodology, Writing – review. Mauro Chierici Lopes: Methodology, Investigation, Writing, Resources.

References and Notes

[1] Xu, Q.; Zhao, T. S. *Prog. Energy Combust. Sci.* **2015**, *49*, 40. [Crossref]

[2] Shen, Y. *Energy* **2014**, *74*, 795. [Crossref]

[3] May, G. J.; Davidson, A.; Monahov, B. *J. Energy Storage* **2018**, *15*, 145. [Crossref]

[4] Jung, J.; Zhang, L.; Zhang, J. Lead-acid battery technologies: Fundamentals, materials and applications. Boca Raton: CRC Press, 2016.

[5] Li, Y.; Shen, Z.; Ray, A.; Rahn, C. D. *J. Power Sources* **2014**, *268*, 758. [Crossref]

[6] Pilatowicz, G.; Budde-Meiwes, H.; Kowal, J.; Sarfert, C.; Schoch, E.; Konigsmann, M.; Sauer, D. U. *J. Power Sources* **2016**, *331*, 348. [Crossref]

[7] Murariu, T.; Morari, C. *J. Energy Storage* **2019**, *21*, 87. [Crossref]

[8] Wassiliadis, N.; Adermann, J.; Frericks, A.; Pak, M.; Reiter, C.; Lohmann, B.; Lienkamp, M. *J. Energy Storage* **2018**, *19*, 73. [Crossref]

[9] Zahid, T.; Xu, K.; Li, W.; Li, C.; Li, H. *Energy* **2018**, *162*, 871. [Crossref]

[10] Vasebi, A.; Partovibakhsh, M.; Bathaee, S. M. T. *J. Power Sources* **2007**, *174*, 30. [Crossref]

[11] Zhang, Y.; Du, X.; Salman, M. *Electr. Power Energy Syst.* **2017**, *85*, 178. [Crossref]

[12] Surendar, V.; Mohankumar, V.; Anand, S.; Prasanna, V. D. *Proced. Technol*. **2015**, *21*, 264. [Crossref]

[13] Kalawoun, J.; Biletska, K.; Suard, F.; Montaru, M. *J. Power Sources* **2015**, *279*, 694. [Crossref]

[14] Tang X.; Gao F.; Zou C.; Yao K.; Hu W.; Wik T. *Appl Energy* **2019**, *238*, 423. [Crossref]

[15] Mesbahi, T.; Khenfri, F.; Rizoug, N.; Chaaban, K.; Bartholomeus, P.; Le Moigne, P. *Electr. Power Syst. Res*. **2016**, *131*, 195. [Crossref]

[16] Omar, N.; Van den Bossche, P.; Coosemans, T.; Van Mierlo, J. *Energies* **2013**, *6*, 5625. [Crossref]

[17] Doerffel, D.; Sharkh, S. A. *J. Power Sources* **2006**, *155*, 395. [Crossref]

[18] Galushkin, N. E.; Yazvinskaya, N. N.; Galushkin, D. N. *Int. J. Electrochem. Sci*. **2019**, *14*, 2874. [Link]

[19] Manenti, A.; Onori, S.; Guezennec, Y. Abstract of 18th The International Federation of Automatic Control (IFAC) - A New Modeling Approach to Predict 'Peukert Effect' for Lead Acid Batteries, Milano, Italy, 2011. [Crossref]

[20] Hausmann, A.; Depcik, C. *J. Power Sources* **2013**, *235*, 148. [Crossref]

[21] Cugnet, M.; Dubarry, M.; Liaw, B. Y. *ECS Trans.* **2010**, *25*, 223. [Link]

[22] Vervaet, A. A. K.; Baert, D. H. J. *Electrochim. Acta* **2002**, *47*, 3297. [Crossref]

[23] D'Alkaine, C. V.; Carubelli, A.; Fava, H. W.; Sanhueza, A. C. *J. Power Sources* **1995**, *53*, 289. [Crossref]

[24] Nebl, C.; Steger, F.; Schweiger, H. G. *Int. J. Electrochem. Sci*. **2017**, *12*, 4940. [Link]

[25] Song, S. US pat. 5,830,595 1998. [Link]

[26] Cugnet, M.; Laruelle, S.; Grugeon, S.; Sahut B.; Sabatier, J.; Tarascon, J.; Oustaloupc, A. *J. Electr. Soc.* **2009**, *156*, A974. [Link]

[27] Bode, H. Lead-acid batteries. New York: John Wiley & Sons, 1977.

[28] Johnston, D.C. *Phys Rev B*. **2006**, *74*, 184430-1. [Crossref]

How to cite this article

Vicari, L. A.; Lima, V. A.; Moraes, A. S.; Lopes, M. C. *Orbital: Electron. J. Chem.* **2021**, *13*, 392. DOI: http://dx.doi.org/10.17807/orbital.v13i5.155